This article was downloaded by:[Northwestern University]
On: 30 July 2008
Access Details: [subscription number 788774864]
Publisher: Taylor & Francis
Informa Ltd Registered in England and Wales Registered Number: 1072954
Registered office: Mortimer House, 37-41 Mortimer Street, London W1T 3JH, UK

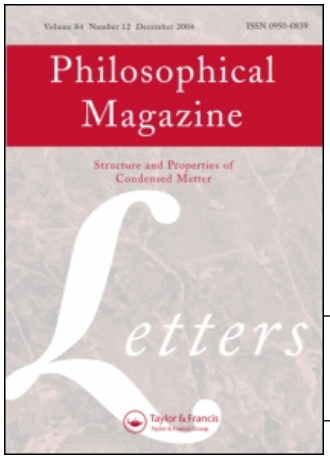

Philosophical Magazine Letters
Publication details, including instructions for authors and subscription information:
http://www.informaworld.com/smpp/title~content=t713695410

Design of micro-nanoscale bio-inspired hierarchical materials

Nicola M. Pugno [a]; Alberto Carpinteri [a]
[a] Department of Structural Engineering, Politecnico di Torino, Torino, Italy

First Published: June 2008

To cite this Article: Pugno, Nicola M. and Carpinteri, Alberto (2008) 'Design of micro-nanoscale bio-inspired hierarchical materials', Philosophical Magazine Letters, 88:6, 397 — 405

To link to this article: DOI: 10.1080/09500830802089843
URL: http://dx.doi.org/10.1080/09500830802089843

PLEASE SCROLL DOWN FOR ARTICLE

Full terms and conditions of use: http://www.informaworld.com/terms-and-conditions-of-access.pdf

This article maybe used for research, teaching and private study purposes. Any substantial or systematic reproduction, re-distribution, re-selling, loan or sub-licensing, systematic supply or distribution in any form to anyone is expressly forbidden.

The publisher does not give any warranty express or implied or make any representation that the contents will be complete or accurate or up to date. The accuracy of any instructions, formulae and drug doses should be independently verified with primary sources. The publisher shall not be liable for any loss, actions, claims, proceedings, demand or costs or damages whatsoever or howsoever caused arising directly or indirectly in connection with or arising out of the use of this material.

Philosophical Magazine Letters
Vol. 88, No. 6, June 2008, 397–405

Taylor & Francis
Taylor & Francis Group

Downloaded By: [Northwestern University] At: 08:12 30 July 2008

Design of micro-nanoscale bio-inspired hierarchical materials

Nicola M. Pugno* and Alberto Carpinteri

Department of Structural Engineering, Politecnico di Torino, Torino, Italy

(*Received 19 October 2006; final version received 30 March 2008*)

In this article two mathematical models, force- or energy-based, are proposed for the design of nanoscale bio-inspired hierarchical materials, considering strong or weak interfaces, respectively. Simple formulas describing the dependence of strength, toughness and stiffness on the considered size scale are derived, taking into account toughening biomechanisms. A simple experimental comparison on a new two-level hierarchical grained material is also discussed.

1. Introduction

Biological materials exhibit several levels of hierarchy, from nano- to macroscale. For instance, seashells have two or three orders of lamellar structures, and bone, similarly dentin, has seven orders of hierarchy [1]. These nanoscale bio-materials consist of hard and strong mineral structures embedded in a soft and tough protein matrix. In bone and dentin, the mineral platelets are $\sim$3 nm thick, whereas in shells of $\sim$300 nm, and are very slender. With this hard and soft nano-hierarchical slender texture, nature seems to suggest a key for optimizing materials with respect to both strength and toughness, without losing stiffness [2]. Even if hierarchical materials are recognized to possess a fractal-like topology [3], only a few engineering models explicitly considering their complex structure have appeared in the literature (see [2,4] and related references). In this article an alternative and concise mathematical model is presented. Additional considerations are reported in the Appendix.

2. Strong interfaces: force equilibrium

Strength, toughness and stiffness of materials are measured by tensile tests. Imagine a virtual tensile test on a hierarchically fibre-reinforced bar [2]. The bar's cross section, composed of hard inclusions assumed here to be perfectly embedded in a soft matrix (strong interfaces), is schematized in Figure 1.

The smallest units, at the levels N (number of considered hierarchical level), are assumed to be scale-invariant and related to the theoretical material strengths of the hard and soft phases, respectively, σ_h and σ_s, where usually $\sigma_h \gg \sigma_s$. Each inclusion at the level

*Corresponding author. Email: nicola.pugno@polito.it

ISSN 0950–0839 print/ISSN 1362–3036 online
© 2008 Taylor & Francis
DOI: 10.1080/09500830802089843
http://www.informaworld.com

Downloaded By: [Northwestern University] At: 08:12 30 July 2008

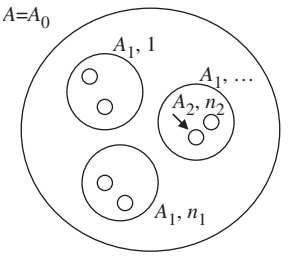

Figure 1. Cross section of a hierarchical bar.

$k+1$ contains n_k smaller ones, each of them with cross-sectional area A_k. Thus, the total number of inclusions at the level k is $N_k = \prod_{j=1}^{k} n_j$, having volumetric fraction $\phi_k = \prod_{j=1}^{k} \varphi_j$. Note that $\varphi_k = (n_k A_k / A_{k-1})$ represents the cross-sectional fraction of the inclusions at the level $k+1$ in the inclusions at the level k.

The *equilibrium equation* is $F \equiv A\sigma_C = F_h + F_s = N_k A_k \sigma_{hk} + (A - N_k A_k)\sigma_{sk} = N_N A_N \sigma_{hN} + (A - N_N A_N)\sigma_{sN}$, $\forall k$, where F is the critical applied force, F_h and F_s are the forces carried by the hard and the soft phases, respectively, $A \equiv A_0$ is the cross-sectional area of the bar, σ_C is its strength, $\sigma_{hN} \equiv \sigma_h$, $\sigma_{hk} \equiv \sigma_s$ ($\forall k$), and the subscript k refers to the quantities at the level k.

Natural optimization suggests nearly self-similar structures [5], for which $n_k = n$ and $\varphi_k = \varphi$, thus k-independent numbers and fractions; accordingly $N_k = n^k$. Since the inclusions present a fractal distribution [6], we expect $F_h \propto R^D$ where $R = A^{1/2}$ is a characteristic size and D is a constant, the so-called "fractal dimension"; the constant of proportionality can be deduced noting that $F_h(A = A_N) = A_N \sigma_{hN}$, and thus $F = \sigma_{hN} R_N^{2-D} R^D$. Accordingly, from $F_h = \sigma_{hN} R_N^{2-D} R^D = \sigma_{hN} n^N R_N^2$, we derive

$$N = D \frac{\ln R/R_N}{\ln n}, \tag{1}$$

which defines the number of hierarchical levels that we need to design an object of characteristic size R. Equation (1) shows that only few hierarchical levels are required for spanning several orders of magnitude in size. For example, for a nanostructured hierarchical "universe", considering for R its actual radius, i.e., $R \approx 10^{26}$ m, for the smallest units a radius of 1 nm, i.e., $R_N \approx 10^{-9}$ m, $n = 5$ and $D = 2$ would result in only 100 hierarchical levels.

The scaling exponent D can be determined noting that $N_N A_N = A\phi$, where $\phi \equiv \phi_N = \varphi^N$ represents the macroscopic (at level 0) cross-sectional fraction of the hard inclusions. Thus, we derive $R/R_N = (n/\varphi)^{N/2}$. Introducing this result into Equation (1) provides the fractal exponent, as a function of well-defined physical quantities:

$$D = \frac{2 \ln n}{\ln n - \ln \varphi}. \tag{2}$$

Note that D represents the fractal dimension of the inclusions, i.e., of a lacunar two-dimensional domain in which the soft matrix is considered as empty [7,8]; for example, the dimension of the well-known Sierpinski carpet (Figure 2) is $D = 1.89$.

Downloaded By: [Northwestern University] At: 08:12 30 July 2008

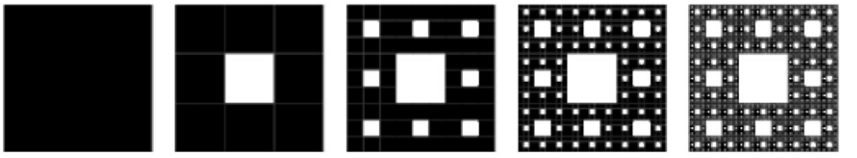

Figure 2. Sierpinski carpet ($D = 1.89$) at different levels of observation. It corresponds to a deterministic hierarchical bar in which the empty space is the soft matrix, and the complementary zones are the hard inclusions.

Since $\sigma_{hN} n^N R_N^2 = \sigma_{hN} R_N^{2-D} R^D$ and $R/R_N = (n/\varphi)^{N/2}$, we derive:

$$\phi = \varphi^N = \left(\frac{R}{R_N}\right)^{D-2}. \tag{3}$$

Thus, from the equilibrium equation, a scaling of the strength is predicted:

$$\sigma_C = \sigma_h \varphi^N + \sigma_s (1 - \varphi^N) = \sigma_h \left(\frac{R}{R_N}\right)^{D-2} + \sigma_s \left(1 - \left(\frac{R}{R_N}\right)^{D-2}\right). \tag{4}$$

Noting that $n > 1$ and $\varphi < 1$, we deduce $0 < D < 2$ and thus Equation (4) predicts that "smaller is stronger" ($\sigma_h \gg \sigma_s$).

On the other hand, the *energy balance* implies $W \equiv AG_C = W_h + W_s = N_k A_k G_{hk} + (A - N_k A_k) G_{sk} = N_N A_N G_{hN} + (A - N_N A_N) G_{sN}$, $\forall k$, where W, W_h, W_s are, respectively, the dissipated fracture energies in the bar, hard and soft phases, and G_C, $G_{hN} \equiv G_h$, $G_{sk} \equiv G_s$ ($\forall k$) are the fracture energies per unit area of the bar, hard and soft phases, respectively; usually $G_h \ll G_s$. Accordingly, the fracture energy scales as:

$$G_C = G_h \varphi^N + G_s \left(1 - \varphi^N\right) = G_h \left(\frac{R}{R_N}\right)^{D-2} + G_s \left(1 - \left(\frac{R}{R_N}\right)^{D-2}\right). \tag{5}$$

And thus "larger is tougher". In the following, toughening mechanisms will be introduced in the model.

On the other hand, the *compatibility equation* implies (bars in parallel): $K \equiv EA = K_h + K_s = N_k A_k E_{hk} + (A - N_k A_k) E_{sk} = N_N A_N E_{hN} + (A - N_N A_N) E_{sN}$, $\forall k$, where K, K_h, K_s, are, respectively, the "elastic" force of the bar, hard and soft phases, and E, $E_{hN} \equiv E_h$, $E_{sn} \equiv E_s$ are the Young's moduli of the bar, hard and soft phases, respectively. Accordingly, Young's modulus scales as:

$$E = E_h \varphi^N + E_s \left(1 - \varphi^N\right) = E_h \left(\frac{R}{R_N}\right)^{D-2} + E_s \left(1 - \left(\frac{R}{R_N}\right)^{D-2}\right). \tag{6}$$

Since, usually, $E_h \gg E_s$, "smaller is stiffer".

Equations (4–6) show that at the smaller size scales the inclusions are dominating, whereas at the larger size scales the matrix dominates. These equations present the same self-consistent form: in fact, regarding the generic property X (σ_C, G_C or E) at the level $N-1$, $X_{N-1} = X_h \varphi + X_s (1 - \varphi)$. Thus, at the level $N-2$, $X_{N-2} = X_{N-1} \varphi + X_s (1 - \varphi) = X_h \varphi^2 + X_s (1 - \varphi^2)$ and iterating $X \equiv X_0 = X_h \varphi^N + X_s (1 - \varphi^N)$, as described

Downloaded By: [Northwestern University] At: 08:12 30 July 2008

by Equations (4–6). In addition, it is clear that the scaling laws predicted by Equations (4–6) are particularly reasonable, since they predict two asymptotic behaviours for macro- and nanosize scales. Note that for a three-dimensional architecture (i.e., particle inclusions and not longitudinal fibres) for which also the third dimension plays a role, in the stiffness of Equation (6) the factor 2 must be replaced by 3, φ becomes the volume fraction rather than the cross-sectional fraction, and D is deduced from Equation (2) considering again the factor 3 instead of 2; this is true if we consider valid the rule of mixture of Equation (6) also for a nonparallel architecture.

Then, the fracture toughness can be derived as $K_C = (G_C E)^{1/2}$, whereas the hardness $H \propto \sigma_C$ formally making the substitution $\sigma_C \to H$ in Equation (4). Note that the important equality (3) would allow us to derive scaling laws from "rules of mixture", also in different systems and for different properties, e.g., the friction coefficient.

Finally, for quasi-fractal hierarchy, described by $n(R)$ and $\varphi(R)$ weakly varying with the size R, a function $D(R)$ should be considered in Equations (4–6), as deducible from Equation (2).

3. Weak interfaces: energy balance

In the presence of weak interfaces, the energy will mainly be dissipated on them during delamination, and the interfaces are thus expected to play the key role. Following [9] we assume that the dissipated energy W_{tot} is proportional to the total surface area A_{tot} of the interfaces at the fractured cross section, and not to the nominal cross-sectional area A. The gain in the energy dissipation imposed by the presence of hierarchy is thus given by [10]:

$$\frac{W_{tot} - W}{W} = \frac{A_{tot} - A}{A} = \frac{2\lambda}{R^2}\sum_{k=1}^{N} N_k R_k^2 = 2\lambda \sum_{k=1}^{N} \phi_k,$$

$$\text{for } \varphi_k = \varphi \Rightarrow \phi_k = \varphi^k \Rightarrow \sum_{k=1}^{N} \phi_k = \frac{\varphi - \varphi^{N+1}}{1 - \varphi} \tag{7}$$

where for spherical grains (0D), $\lambda = 2$, whereas for 1D- or 2D-inclusions, $\lambda = L_k/R_k$ represents their slenderness. Note the dramatic role played by a large value of λ, as observed in the mineral platelets of nacre, bone or dentine materials, in enlarging the composite toughness. A similar mechanism is discussed in the next section for strong interfaces.

Thus, the gain in the fracture energy imposed by hierarchy (with a number of level explicitly shown here as superscripts of the symbols) is predicted to be

$$\frac{G_C^{(N)}}{G_C^{(0)}} = 1 + 2\lambda \sum_{k=1}^{N} \phi_k. \tag{8}$$

For Young's modulus, from Equation (6) we derive:

$$\frac{E^{(N)}}{E^{(0)}} = \phi_N + \frac{E_s}{E_h}(1 - \phi_N). \tag{9}$$

Downloaded By: [Northwestern University] At: 08:12 30 July 2008

Thus, for the fracture toughness [$K_C = (G_C E)^{1/2}$] we expect:

$$\frac{K_C^{(N)}}{K_C^{(0)}} = \sqrt{\left[1 + 2\lambda \sum_{k=1}^{N} \phi_k\right]\left[\phi_N + \frac{E_s}{E_h}(1 - \phi_N)\right]}. \tag{10}$$

Assuming the characteristic crack length to be proportional to $R_N^{-1/2+\alpha} R^{-\alpha}$ [9], where usually $0 \le \alpha \le 1/2$ (even if $\alpha > 1/2$ simply describes an inversion, often observed, of the classical Hall–Petch law), the strength $\sigma_C^{(N)} \propto K_C^{(N)} R_N^{-1/2+\alpha} R^{-\alpha}$ or hardness are predicted to be:

$$\frac{\sigma_C^{(N)}}{\sigma_C^{(0)}} = \frac{H^{(N)}}{H^{(0)}} = \left(\frac{R}{R_N}\right)^{1/2-\alpha} \sqrt{\left[1 + 2\lambda \sum_{k=1}^{N} \phi_k\right]\left[\phi_N + \frac{E_s}{E_h}(1 - \phi_N)\right]}. \tag{11}$$

As an example, we can treat the experimental results on double-cemented WC-Co [11], a new two-level hierarchical grained material, for which $\varphi_1 = 0.73$, $\varphi_2 = 0.94$, with particle diameter $d_1 = 200\,\mu\text{m}$ and sub-particle diameter $d_2 = 1 - 6\,\mu\text{m}$. The experimental mechanical tests were performed on standard (ASTM-B406) rectangular bars having volume $V = 0.500 \times 0.625 \times 1.875 = 0.586\,\text{cm}^3$. We assume spherical grains ($\lambda = 2$). Accordingly $n_1 = \varphi_1 V/(\pi/6)d_1^3 = 102,125$ is the predicted number of mesoparticles in the total volume, whereas $n_2 = \varphi_2 d_1^3/d_2^3 = 34{,}815 - 7{,}520{,}000$ is that of the microparticles inside a mesoparticle. Thus the specimen is composed of several billions of microparticles. According to Equation (8) the gain in the fracture toughness energy is $G_C^{(1)}/G_C^{(0)} = 1 + 4\varphi_1 = 3.92$, $G_C^{(2)}/G_C^{(0)} = 1 + 4(\varphi_1 + \varphi_1\varphi_2) = 6.66$, thus $G_C^{(2)}/G_C^{(1)} = 1.70$. Assuming $E_s \ll E_h$, $E^{(1)}/E^{(0)} = \varphi_1 = 0.73$, $E^{(2)}/E^{(0)} = \varphi_1\varphi_2 = 0.69$ and thus $E^{(2)}/E^{(1)} = 0.95$. Accordingly

$$\frac{K_C^{(2)}}{K_C^{(1)}} = \sqrt{\frac{G_C^{(2)}}{G_C^{(1)}}\frac{E^{(2)}}{E^{(1)}}} = 1.27,$$

close to the experimental, even if scattered, observations [11]. Regarding the strength or hardness we expect for $\alpha = 0$ (crack length proportional to the grain size) $\sigma_C^{(2)}/\sigma_C^{(1)} = H^{(2)}/H^{(1)} = (K_C^{(2)}/K_C^{(1)})(d_1/d_2)^{1/2} = 7 - 20$ quite unreasonable, for $\alpha = 1/2$ (crack length proportional to the structural size) $\sigma_C^{(2)}/\sigma_C^{(1)} = H^{(2)}/H^{(1)} = K_C^{(2)}/K_C^{(1)} = 1.27$, whereas for $\alpha = 0.6$ $\sigma_C^{(2)}/\sigma_C^{(1)} = H^{(2)}/H^{(1)} = (K_C^{(2)}/K_C^{(1)})(d_2/d_1)^{0.1} = 0.75 - 0.89$. Since, experimentally, $H^{(2)}/H^{(1)}$ was observed to be slightly smaller than the unity, we deduce an inversion of the classical Hall–Petch law.

4. Toughening mechanisms for strong interfaces: viscoelasticity, plasticity and crack deflection or bridging

Introducing a Young's modulus we have implicitly assumed linear elasticity. For a more realistic behaviour of the matrix, we should consider viscoelasticity, often observed in bio-tissues. If $\mu_v \equiv (E^0 - E^\infty)/E^\infty$, with E^0, E^∞ as short- and long-time elastic moduli, respectively ($E^0 \ge E^\infty$, where the equality is valid for linear elasticity), the effective fracture energy becomes $G_s^+ = (1 + \mu_v)G_s$. The parameter μ_v represents an enhancement factor for fracture energy dissipation due to the viscoelastic properties of the medium, e.g., for

Downloaded By: [Northwestern University] At: 08:12 30 July 2008

bone $\mu_v \approx 4$ or for shell $\mu_v \approx 1.5$ [12]. Including plasticity, if μ_p represents the enhancement factor due to the plastic work during fracture, $G_s^+ = (1+\mu)G_s$, where $\mu = \mu_v + \mu_p$. The factor μ_p can be estimated for blunt cracks as $\mu_p = \rho/2a$ [13], ρ being the tip radius and a being the "fracture quantum", a material/structural parameter.

According to the previous analysis and Figure 1, the fracture surface is assumed to be planar. On the other hand, the inclusions could serve as hard structures to deflect the crack path or as crack-bridging elements, assuming strong interfaces. For weak interfaces, the inclusions will be pulled out after fracture, incrementing the dissipated energy (see previous section) in a fashion similar to the other mechanisms (if the fracture of the matrix is assumed to be similar to that of the interface; it is evident that this hypothesis can be easily removed). To model crack deflection we simply assume the two-dimensional scheme reported in Figure 3, which is a lateral view of the crack surface of Figure 1. According to this scheme, $G_s^{++} l = G_s^+ (l + nh)$, where l is the nominal crack length, n is the number of inclusions along l and h is their height. Noting that $\varphi = nt/l$, with t the thickness of the inclusions, and that $\lambda = h/t$ is their slenderness, the effective fracture energy becomes $G_s^{++} = (1 + \lambda\varphi)G_s^+$. Thus, this toughening mechanism can also enhance the effective fracture energy G_s^{++} ($\mu \approx \varphi \approx 1$; $\lambda \gg 1$) by several orders of magnitude with respect to the intrinsic fracture energy of the matrix G_s. This explains why the shape of mineral crystals is found to be very anisometric (platelets, [12]), no matter if the interfaces are strong or weak: the anisometry is larger for bone and dentin (platelets 3 nm thick and up to 100 nm long) as well as for enamel (15–20 nm thick, 1000 nm long) than for nacre (i.e., see shells, 200–500 nm thick and 5–8 μm long). For details on the hierarchical bone structure, see [14]. Thus, Equation (5) in general has to be considered with the substitutions:

$$G_s \to (1+\mu)(1+\lambda\varphi)G_s \tag{12a}$$

$$G_h \to 0 \tag{12b}$$

since, in this case, no dissipation occurs in the hard phase.

Furthermore, a soft matrix activates shear mechanisms rather than longitudinal ones, according to the tension-shear chain model recently proposed [12]. Since, in this case, matrix does not carry tensile load, the substitution

$$\sigma_s \to 0 \tag{13}$$

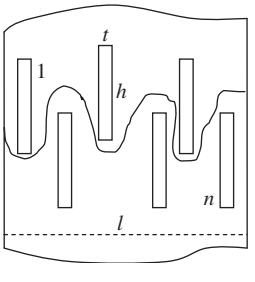

Figure 3. Lateral view of the crack surface: toughening mechanism.

Downloaded By: [Northwestern University] At: 08:12 30 July 2008

should be considered in Equation (4). Considering a linear variation of the shear stress (but stress concentration factors could be included [15]) with a maximum value τ implies a maximum normal stress σ in the platelet equal to $\lambda\tau$ [12]. Thus, load transfer requires $\lambda\tau_s > \sigma_C$ where τ_s is the shear strength of the matrix (or, strictly speaking, of the matrix/inclusion interface); this shows that low values of τ_s are compensated in nature by high values of slenderness λ. Note that, according to [12], an in-series tension/shear rather than an in-parallel tension architecture, as considered in Equation (6), emerges. However, their asymptotic behaviours (for realistic sufficiently large size-scales R) are identical if in Equation (6) Young's modulus of the matrix is assumed to be negligible, i.e.:

$$E_s \to 0 \tag{14}$$

5. Size and shape of "flaw-tolerant" 1D- and 2D-inclusions

Let us consider for the sake of simplicity the Griffith's problem. According to quantized fracture mechanics [13] the failure stress is predicted to be $\sigma_f = (G_C E/(\pi l + a/2))^{1/2}$ (see [13] for details), where $2l$ is the crack length and a is the fracture quantum (linear elastic fracture mechanics, LEFM, assumes $a = 0$). Thus, a "flaw tolerance" is expected to take place for crack lengths $2l$ smaller than a and surely in platelets with thickness $t \approx a$. The fracture quantum a can be estimated noting that $\sigma_f(l = 0) = \sigma_C$, and thus the platelet thickness or grain size for flaw tolerance is

$$t_N \approx \frac{G_C^{(N)} E^{(N)}}{\sigma_C^{(N)2}} \tag{15}$$

similar to what has previously been deduced [16,12]. This characteristic length also represents the optimal diameters for hierarchical grains (or grain size; see the Appendix). Inserting Equations (4), (5) and (6) or (8), (9) and (11) into Equation (15) defines the thicknesses of the inclusions at all the hierarchical levels for flaw tolerance.

In addition, to reach the failure simultaneously in the soft and hard phases, the following equation for the slenderness at a given hierarchical level must hold (see previous section):

$$\lambda_N \approx \frac{\sigma_C^{(N)}}{\tau_s} \tag{16}$$

Finally, nature seems to optimize structures by imposing the ratio between fractal D and Euclidean nominal dimensions D according to $D/\mathrm{D} = \mathrm{D}/(\mathrm{D}+1)$ [17], e.g., for $\mathrm{D} = 3$, $D/3 = 3/4$ [5]. Thus $D/2 \approx 2/3$, from Equation (2), and the optimum would imply

$$D_{opt} \approx 4/3, \text{ or } (\varphi n^{1/2})_{opt} \approx 1 \tag{17}$$

The fractal dimension of the inclusions, according to Equation (17), is intermediate between those of a Euclidean line and surface.

Equation (15) defines the optimal platelet thicknesses for flaw tolerant, Equation (16) the optimal platelet slenderness to have a uniform strength in both the phases and Equation (17) the relation between their number and cross-sectional area fraction for having an optimal fractal dimension.

Downloaded By: [Northwestern University] At: 08:12 30 July 2008

6. Conclusions

The developed mathematical model, summarized in the numbered equations, allows us to preliminary design nanoscale bio-inspired hierarchical materials, by following a bottom-up or top-down procedure. The complexity of the problem has imposed a simplified treatment with associated limitations; nevertheless, the model could be useful for preliminary designing micro- or nanostructured hierarchical materials.

Acknowledgement

The authors are supported by the "Bando Ricerca Scientifica Piemonte 2006" – BIADS: Novel biomaterials for intraoperative adjustable devices for fine-tuning of prostheses shape and performance in surgery.

References

[1] J.D. Currey, Proc. R. Soc. B 196 (1977) p.443.
[2] N. Pugno, Nanotechnology 17 (2006) p.5480.
[3] R. Lakes, Nature 361 (1993) p.511.
[4] H. Gao, Int. J. Fract. 138 (2006) p.101.
[5] J.H. Brown and G.B. West, *Scaling in Biology*, Oxford University Press, Oxford, 1999.
[6] A. Carpinteri and N. Pugno, Nat. Mater. 4 (2005) p.421.
[7] A. Carpinteri, Mech. Mater. 18 (1994) p.89.
[8] A. Carpinteri, Int. J. Solids Struct. 31 (1994) p.291.
[9] A. Carpinteri and N. Pugno, Rev. Adv. Mater. Sci. J. 10 (2005) p.320.
[10] N. Pugno, J. Physics – Cond. Matt. 19 (2007) 395001.
[11] Z.Z. Fang, A. Griffo, B. White et al., Int. J. Refract. Metals Hard Mater. 19 (2001) p.453.
[12] B. Ji and H. Gao, J. Mech. Phys. Solids 52 (2004) p.1963.
[13] N. Pugno and R. Ruoff, Philos. Mag. 84 (2004) p.2829.
[14] O. Akkus, Y.N. Yeni and N. Wesserman, Crit. Rev. Biomed. Eng. 32 (2004) p.379.
[15] N. Pugno and A. Carpinteri, J. Appl. Mech. 70 (2003) p.832.
[16] A. Carpinteri, Eng. Fract. Mech. 16 (1982) p.467.
[17] R.B. Banavar, A. Maritan and A. Rinaldo, Nature 399 (1999) p.130.
[18] A. Lammer, Mater. Sci. Techn. 4 (1988) p.949.
[19] R.A. Masamura, P.M. Hazzledine and C.S. Pande, Acta Mater. 46 (1998) p.4527.
[20] J. Gurland, Trans. Metall. Soc. AIME 227 (1963) p.1146.

Appendix – Optimal grain size

Let us consider a matrix embedding (not hierarchical) grains with a mean diameter d. The characteristic crack length is statistically expected to be of the order of $2l \approx d$ [18]; thus $\sigma_f \approx [2G_C E/(\pi d + a)]^{1/2}$. Accordingly, for large grain sizes $\sigma_f \propto d^{-1/2}$, as described by the well-known Hall–Petch law, whereas for small grain sizes a deviation from this law is expected, i.e. $\sigma_f \propto d^0$. This deviation is observed in experiments and is erroneously assumed to take place around a grain size of 10 nm (see the discussion [19]). The same transition has been recently derived [9], extending the fractal approach for size effects [6] to grains. The grain size corresponding to the transition, or even to the inversion of the Hall–Petch law (in the case of a positive exponent, for example, due to a fracture energy $G_C(d)$ increasing with the grain size d), represents an optimal value for flaw tolerance. According to our simple considerations, and in contrast to the common assumption of a "universal" value of 10 nm, we expect the optimal grain size depending on the

material properties of the mixture but assumed to be very fine grained, i.e. of the amorphous counterpart (i.e. $d \to 0$, since $\sigma_C = \sigma_f(d=0)$) and containing the given grain content ϕ (e.g., in the form suggested by Equations (4–6) with $\varphi^N = \phi$), i.e. $d_{opt} \approx G_C(\phi)E(\phi)/\sigma_C^2(\phi) \approx K_{IC}^2(\phi)/\sigma_C^2(\phi)$. Let us observe that, for $K_{IC} \approx 10\,\text{MPa}$, if $\sigma_C \approx 100\,\text{GPa}$ we obtain $d_{opt} \approx 10\,\text{nm}$, whereas if $\sigma_C \approx 1\,\text{GPa}$ we obtain $d_{opt} \approx 100\,\mu\text{m}$. We have found some experimental results in the literature that show a deviation from the Hall–Petch law for a ''large'' grain size, i.e. of several microns [18,20], supporting our argument. This optimal grain size could be perhaps applied also in different contexts, e.g., to optimize coating layers.

Downloaded By: [Northwestern University] At: 08:12 30 July 2008